Creation of mortality risk charts using ^{123}I meta-iodobenzylguanidine heart-to-mediastinum ratio in patients with heart failure: 2- and 5-year risk models

Kenichi Nakajima[1]*, Tomoaki Nakata[2], Shinro Matsuo[1], and Arnold F. Jacobson[3]

[1]Department of Nuclear Medicine, Kanazawa University Hospital, 13-1 Takara-machi, Kanazawa 920-8641, Japan; [2]Hakodate Goryoukaku Hospital, Hakodate-City, Japan; and [3]Diagram Consulting, Kihei, HI, USA

Aims	^{123}I meta-iodobenzylguanidine (MIBG) imaging has been extensively used for prognostication in patients with chronic heart failure (CHF). The purpose of this study was to create mortality risk charts for short-term (2 years) and long-term (5 years) prediction of cardiac mortality.
Methods and results	Using a pooled database of 1322 CHF patients, multivariate analysis, including ^{123}I-MIBG late heart-to-mediastinum ratio (HMR), left ventricular ejection fraction (LVEF), and clinical factors, was performed to determine optimal variables for the prediction of 2- and 5-year mortality risk using subsets of the patients ($n = 1280$ and 933, respectively). Multivariate logistic regression analysis was performed to create risk charts. Cardiac mortality was 10 and 22% for the subpopulation of 2- and 5-year analyses. A four-parameter multivariate logistic regression model including age, New York Heart Association (NYHA) functional class, LVEF, and HMR was used. Annualized mortality rate was <1% in patients with NYHA Class I–II and HMR ≥ 2.0, irrespective of age and LVEF. In patients with NYHA Class III–IV, mortality rate was 4–6 times higher for HMR < 1.40 compared with HMR ≥ 2.0 in all LVEF classes. Among the subset of patients with b-type natriuretic peptide (BNP) results ($n = 491$ and 359 for 2- and 5-year models, respectively), the 5-year model showed incremental value of HMR in addition to BNP.
Conclusion	Both 2- and 5-year risk prediction models with ^{123}I-MIBG HMR can be used to identify low-risk as well as high-risk patients, which can be effective for further risk stratification of CHF patients even when BNP is available.
Keywords	^{123}I meta-iodobenzylguanidine • chronic heart failure • prognosis • risk chart • cardiac death • prediction model

Introduction

Cardiac uptake of ^{123}I-meta-iodobenzylguanidine (MIBG) has been shown to be a potent prognostic marker in patients with chronic heart failure (CHF). Compared with conventional clinical parameters, the independent and additive value of MIBG has been demonstrated in single-centre and multicentre studies.[1–6] Low heart-to-mediastinum ratio (HMR), a simple but widely used index of cardiac sympathetic nerve integrity, is strongly related to poor prognosis including cardiac death, life-threatening arrhythmias, and sudden cardiac death. Studies examining therapeutic interventions have also demonstrated that HMR was improved in patients with good response and improved cardiac functional status.[7–9]

Most studies have used HMR as a prognostic index based upon hazard ratios among different patient groups. While risk for all-cause and cardiac mortality has been related to HMR, the contribution of this measure to prediction of absolute mortality rates has not yet been established.[4,10] In addition, while HMR may improve in

response to CHF treatment, the degree to which a change of HMR, though statistically significant, actually influences mortality risk has not been clearly shown. It also remains to define an appropriate population for whom ^{123}I-MIBG is beneficial for clinical decision-making.[11,12]

We therefore have developed risk models that can directly demonstrate the mortality risk as a per cent unit.[13] By directly converting HMR values into predicted mortality rates, risk stratification of patients into low-, intermediate-, and high-risk groups becomes more straightforward. We created both 2-year and 5-year models with ^{123}I-MIBG imaging to facilitate more flexible risk-based decision-making for the selection of short-term as well as long-term therapeutic strategies.

Methods

Patients

A pooled database created by the collaboration of six prognostic cohort studies was used in this study as described elsewhere.[3] Briefly, the database consisted of 1322 patients registered between 1990 and 2009 (male, $n = 942$), who underwent cardiac ^{123}I-MIBG study at a stable condition of CHF.[14−19] CHF aetiology was 73% non-ischaemic and 27% ischaemic. The mean follow-up time was 6.5 ± 4.1 years (range 0.08−14.6 years). The mean left ventricular ejection fraction (LVEF) was $37 \pm 14\%$ using two-dimensional echocardiography, gated blood-pool study, or gated single-photon emission computed tomography. Mean late HMR was 1.75 ± 0.35. All the studies were approved by the ethics committee or institutional review board in each hospital.

Subset populations for creating 2-year and 5-year models

To provide a complete data set for 2-year analysis, 1280 patients who had definitive 2-year outcomes (death or survival) were included, with those who were alive and censored prior to 2 years excluded (Table 1). Similarly, 933 patients who had information of 5-year outcomes were included for the 5-year analysis. The baseline characteristics did not differ significantly between these groups.

^{123}I-MIBG study

A dose of 111 MBq of ^{123}I-MIBG was used in all studies. Early and late anterior planar images of thorax were obtained 15−30 min (early) and 3−4 h (late), respectively. All participating hospitals used low-energy-type collimators. The HMR, determined from cardiac and upper mediastinal regions of interest, was defined as the ratio of average heart count/pixel divided by mediastinal count/pixel. We used only late HMR in this study, since it showed better discrimination of prognosis than early HMR and washout rate.[3]

Follow-up endpoints

Endpoint was cardiac death including pump-failure death (PFD), sudden cardiac death (SCD), and death from acute myocardial infarction (AMI). Those who had non-cardiac death were dealt with as censored at the time of death.

Multivariate analyses and risk prediction models

Multivariate proportional hazard analysis was performed in both 2- and 5-year sub-populations to find the number of significant variables for predicting cardiac death. Using these significant candidate variables, multivariate logistic regression analysis was performed to determine appropriate number of predictors of cardiac death. The final mortality prediction model was created with parameter estimates calculated by the logistic analysis. This model-based probability (p) could be calculated using the formula of

$$p = \frac{1}{1 + \text{Exp}[-(b(0) + \Sigma(b(i) * x(i)))]},$$

where $b(i)$ was a parameter estimate, and $x(i)$ was a predictor variable.

Creation of risk chart

To clarify characteristics of 2- and 5-year models, risk charts were created with significant variables to allow prediction of cardiac mortality using a unit of %. The variables were classified into several classes as follows. NYHA functional class was divided into I−II and III−IV sub-classes. LVEF was divided into three: EF $\leq$ 35%, 35 < EF < 50%, and EF $\geq$ 50%. HMR was classified into four: <1.4, 1.40−1.69, 1.70−1.99, and $\geq$2.0.

Table I Patient demographics in total and sub-populations for creating models

	Total population	2-year model sub-population	5-year model sub-population	2-year model with BNP	5-year model with BNP
Number	1322	1280	933	491	359
Age (years)	61 ± 13	61 ± 13	61 ± 14	62 ± 14	63 ± 14
Male sex (%)	71	71	71	72	69
NYHA class (% of III and IV)	34	34	34	51[*1]	49[*2]
LVEF (%)	37 ± 14	37 ± 14	36 ± 13	35 ± 11	35 ± 12
^{123}I-MIBG HMR	1.75 ± 0.35	1.75 ± 0.35	1.71 ± 0.33	1.70 ± 0.25	1.68 ± 0.26
BNP (pg/mL)	373 ± 421	381 ± 427	405 ± 451	381 ± 427	405 ± 451
Ischaemic aetiology (%)	27	28	26	24	24
Total follow-up period (years)	6.5 ± 4.1	6.6 ± 4.1	7.7 ± 4.3	4.9 ± 2.2[*3]	5.4 ± 2.4[*4]
Cardiac mortality (n, %)	263, 20	125, 10	205, 22	54, 11	102, 28

NYHA, New York Heart Association; LVEF, left ventricular ejection fraction; HMR, heart-to-mediastinum ratio; BNP, b-type natriuretic peptide.
Statistics between total sub-population versus that for BNP analysis: [*1], $P < 0.0001$ vs. total 2-year data; [*2], $P < 0.0001$ vs. total 5-year data; [*3], $P < 0.0001$ vs. total 2-year data; [*4], $P < 0.0001$ vs. total 5-year data.

Table 2 Causes of cardiac death of patients in 2- and 5-year sub-populations

	2-year model			5-year model		
	n	2-year mortality (%)	Proportion (column %)	*n*	5-year mortality (%)	Proportion (column %)
Sudden cardiac death	38	3	30	61	7	30
Pump-failure death	80	6	64	132	14	64
Acute myocardial infarction death	7	1	6	12	1	6
Total	125	10	100	205	22	100

In the logistic analyis, receiver operating characteristic (ROC) analysis using area under the curve (AUC) was performed to determine an optical threshold together with data histograms. For the calculation of an annualized mortality rate, we assumed that the annual mortality rate was constant during the follow-up period and exponential decrease in surviving patients, which was not simply the death rate divided by the number of years follow-up.

Although b-type natriuretic peptide (BNP) data were available for only 491 patients for the 2-year model and 359 patients for the 5-year model, supplementary logistic multivariate analyses were performed by including BNP data.

Statistics

All the values were expressed as mean $\pm$ standard deviations (SD). Mean values between the two groups were compared using the unpaired *t*-test and analysis of variance. Prevalence values were compared using the χ^2 test. Likelihood ratio test and Pearson statistics were used to evaluate difference in contingency tables. ROC analysis was performed to determine the optimal cut-off values using AUC and model χ^2. Univariate and multivariate proportional hazard analyses were performed to select major significant variables, and the selection of variables with multivariate analysis was based on the forward stepwise method using a *P*-value threshold. Multivariate logistic analysis was used to create logistic models. All analyses were performed using the SAS statistical program package (JMP version 10.0, SAS, Cary, NC, USA). To calculate risk values and charts, Mathematica 10.1 (Wolfram Research Inc., Champaign, IL, USA) was used.

Results

Patient demographics and cardiac mortality

There were no significant differences in patient demographics between 2- and 5-year sub-populations (*Table 1*). Medications did not differ significantly between the two groups for use of β-blockers, angiotensin-converting enzyme inhibitors, angiotensin receptor blockers, and diuretics. In the 2- and 5-year sub-populations, cardiac mortality was 10 and 22%, respectively. Fractions of deaths from SCD, PFD, and AMI did not differ significantly between 2- and 5-year sub-populations (*Table 2*).

The breakdown of cardiac death was compared between the ischaemic and non-ischaemic groups for the 2- and 5-year models (*Figure 1*). In the 2-year sub-population, SCD was the highest (50%) followed by PFD (38%) and AMI death (13%) in the ischaemic group. In contrast, fraction of PFD was the highest (73%) in the
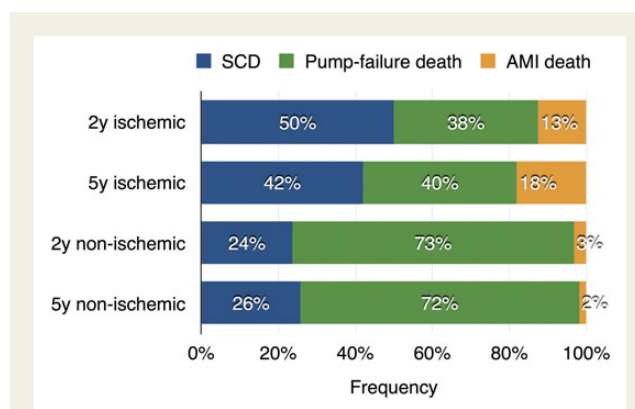

Figure 1 Cause of death in the ischaemic and non-ischaemic CHF patients for 2- and 5-year model groups. SCD, sudden cardiac death; AMI, acute myocardial infarction.

non-ischaemic group. Similar tendency was observed in the 5-year sub-population. Distribution of aetiologies of cardiac death in the ischaemic and non-ischaemic groups differed significantly in both the 2-year (*P* = 0.0010) and the 5-year model groups (*P* < 0.0001).

Multivariate proportional hazard analysis

Based on our previous results using the original databases (*n* = 1,322),[13] five candidates for significant variables were examined. In both 2 and 5-year subsets of the patients, significant variables were NYHA Class I–II and III–IV, MIBG late HMR, age, sex, and LVEF in the order of χ^2 (*Table 3*). The latter four variables were used as continuous variables in this analysis. When CHF aetiology (ischaemic versus non-ischaemic) was included in multivariate analysis, this variable was not a statistically significant predictor of cardiac mortality.

Creation of mortality risk charts using multivariate logistic regression model

Two-year logistic regression model included NYHA class, late HMR, and age as significant variables; LVEF was of borderline significance (*P* = 0.054) (*Table 4*). In the 5-year group, NYHA class, late HMR, age, and LVEF were significant variables.

Mortality risk charts for 2 and 5 years were created for NYHA Class I–II (*Figure 2*) and Class III–IV (*Figure 3*). Considering the consistency between the two model parameters and for comparison of the model characteristics, four variables, including NYHA class,

Table 3 Proportional hazard analysis for 2- and 5-year sub-populations including complete follow-up (mean 6.5 years)

	2-year model			5-year model		
	χ^2	P	Hazard ratio	χ^2	P	Hazard ratio
NYHA class (I, II vs. III, IV)	51.74	<0.0001	2.56	50.39	<0.0001	2.57
^{123}I-MIBG HMR	51.65	<0.0001	0.21	38.80	<0.0001	0.25
Age (years)	19.59	<0.0001	1.02	20.31	<0.0001	1.02
LVEF (%)	14.85	0.0001	0.98	10.76	0.0010	0.98
Male sex	6.20	0.0128	1.43	8.55	0.0035	1.52

Abbreviations are the same as in *Table 1*.

Table 4 Parameter estimates by logistic analysis in the 2- and 5-year models

	Parameter estimate	Standard error	χ^2	P
2-year model				
Intercept	−0.6361	0.7883		
NYHA class (I, II vs. III, IV)	1.3631	0.2143	40.45	<0.0001
^{123}I-MIBG HMR	−1.7961	0.3600	24.90	<0.0001
Age (years)	0.0203	0.0082	6.10	0.0135
LVEF (%)	−0.0168	0.0087	3.72	0.0536
5-year model				
Intercept	0.5941	0.6929		
NYHA class (I, II vs. III, IV)	1.2782	0.1795	50.73	<0.0001
^{123}I-MIBG HMR	−1.9224	0.3354	32.85	<0.0001
Age (years)	0.0216	0.0070	9.45	0.0021
LVEF (%)	−0.0178	0.0077	5.40	0.0201

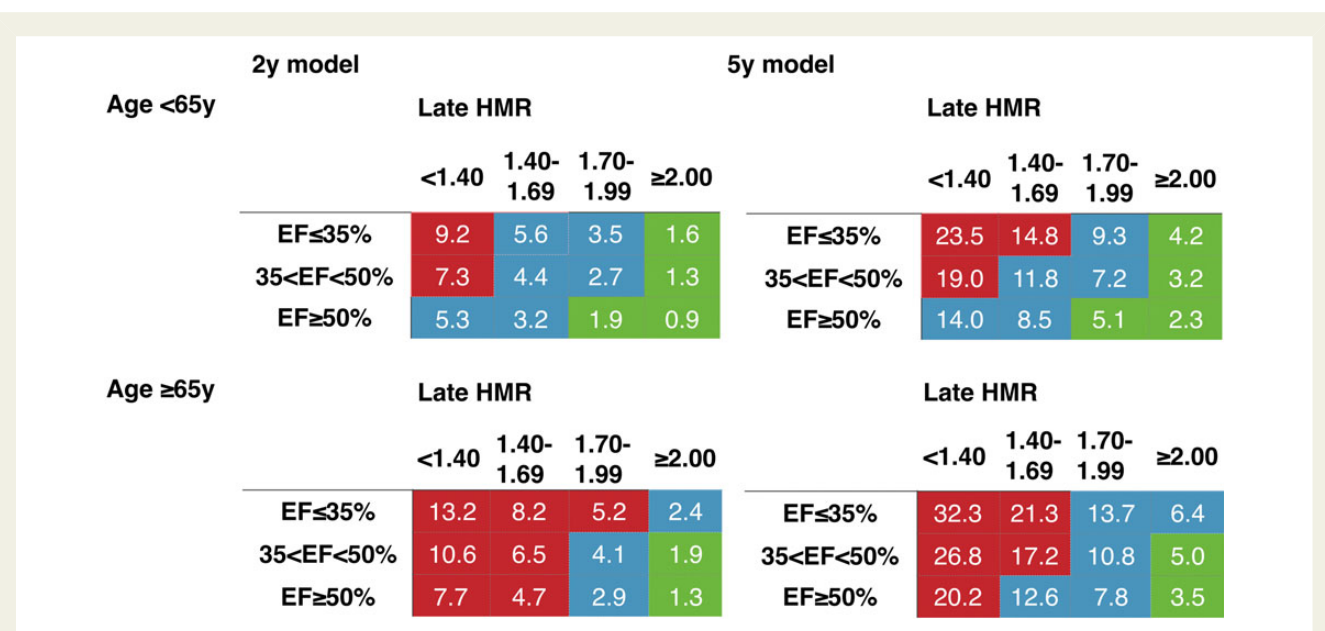Abbreviations are the same as in *Table 1*.

Figure 2 Mortality risk chart using ^{123}I-MIBG HMR, LVEF, and age in patients with NYHA Class I–II. Colours are based on calculated annual cardiac mortality rate using exponential decay of the survival curves: green, <1%; blue, 1.0–2.9% and red, 3.0–9.9%.

Figure 3 Mortality risk chart using ^{123}I-MIBG HMR, LVEF, and age in patients with NYHA Class III−IV. Colours are based on calculated annual cardiac mortality rate using exponential decay of the survival curves: blue, 1.0−2.9%; red, 3.0−9.9%, and purple, ≥ 10%.

^{123}I-MIBG HMR, age, and LVEF, were selected. Since the logistic models were based on continuous variables, average value of each class was used to create both 2- and 5-year risk charts.

In all classes of LVEF, NYHA, and age, the mortality rate was consistently higher in the lower HMR groups in both 2- and 5-year models. In patients with NYHA Class I−II and age < 65 years, annual cardiac mortality rate was <1% if HMR was ≥2.0 in any LVEF ranges and LVEF ≥ 50% with HMR > 1.7 (*Figure 2*). In patients with NYHA I−II and age ≥ 65 years, this low risk was seen only for LVEF ≥ 35% with HMR ≥ 2.0. In patients with NYHA Class III−IV (*Figure 3*), no patients showed annual mortality risk of <1%. However, the total and annual mortality risk in patients with HMR < 1.40 was 4−6 times higher than for HMR ≥ 2.0 in all LVEF ranges.

Mortality risk models including BNP data

Because of the limited number of BNP data available, we included only ^{123}I-MIBG HMR (four categorical groups) and BNP (three categorical groups of 0−199, 200−399, and ≥400 pg/mL) in the models. Odds ratio of BNP was 2.56 and 9.27 for 2- and 5-year models ($P < 0.0001$ for both), respectively, and that of HMR was 1.49 and 3.34 ($P = 0.042$ and 0.019) for 2- and 5-year models, respectively. When compared with the whole 2- and 5-year populations, the sub-populations with BNP data had more frequently NYHA Class III−IV (*Table 1*) and had a higher 5-year mortality ($P = 0.016$), but the other background characteristics were comparable.

In the 2-year model using only BNP data, ROC curve AUC was 0.729 ($\chi^2 = 35$), but it was increased to 0.751 ($\chi^2 = 39$, $P = 0.066$ vs. BNP only) by adding HMR (*Figure 4*). Similarly, in the 5-year model (BNP only), ROC curve AUC significantly increased from 0.756 ($\chi^2 = 35$) to 0.779 by the addition of HMR ($\chi^2 = 74$, $P = 0.016$ vs. BNP only). Even in the same BNP classes, patients

Figure 4 Mortality risk charts including BNP and ^{123}I-MIBG HMR. The colours are based on annualized cardiac mortality rate as indicated in *Figure 3*. Colours are based on calculated annual cardiac mortality rate using exponential decay of the survival curves: blue, 1.0−2.9%; red, 3.0−9.9%, and purple, ≥ 10%.

with HMR < 1.40 showed 2−3 times higher mortality risk compared with those with HMR > 2.0.

Discussion

This study confirmed substantial prognostic value of cardiac ^{123}I-MIBG HMR in both 2- and 5-year mortality risk estimations. Using a four-parameter risk model including HMR and readily

available clinical parameters, CHF patients were successfully stratified into low-, intermediate-, and high-risk probability of cardiac death.

The present study used a large-scale, multiple cohort MIBG database with an average follow-up period of 6.5 years. Previous studies showed different significant mortality predictors depending on clinical backgrounds and study designs, including LVEF, BNP, complications of diabetes, anaemia and chronic kidney disease, and medications.[2,5,18,20–22] In ADMIRE-HF, NYHA functional class, age, LVEF, and HMR were significant variables.[6,10,23] Similarly in meta-analysis performed in Europe, late HMR, sex, LVEF, and NYHA class were significant determinants of lethal events by multivariate analysis.[4] The clinical Seattle Heart Failure Model includes age, sex, NYHA class, body weight, LVEF, systolic blood pressure, and ischaemic aetiology, as well as laboratory data such as haemoglobin and kidney function, and medications and cardiac device treatments.[24] Because of the large number of cardiac mortality risk factors, contribution of each individual factor to final outcomes is difficult to quantify and is likely to limit use of clinical models. In contrast, the three clinical variables used in this study (age, LVEF and NYHA functional class) are readily available and understandable for clinicians.

During more than two decades, a number of studies performed in Japan, Europe, and the North America have demonstrated relatively short-term (2–4 years) prognostic value of ^{123}I-MIBG imaging in CHF patients.[12] Short-term risk prediction is valuable for the selection of treatment, and therapeutic response can be readily judged within 2 years. Patients with CHF, however, are consistently at increased risk for worsening of heart failure, hospitalization, and sudden death. Although recent advances in pharmacological and non-pharmacological treatment in CHF have improved patient survival, there are non-negligible number of patients who do not respond to these treatments. There is a clinical need for both short-term and long-term risk stratification and prediction of overall mortality. Our previous study demonstrated HMR-dependent decreases in survival curves in 1322 CHF patients during a 10-year interval.[3] Since current decisions that have long-term implications, such as use of implantable devices and listing for heart transplantation, require longer term risk stratification, additive values of ^{123}I-MIBG for both 2- and 5-year risk estimation are evident on the risk charts. For example, in patients with age $\geq$ 65 years, NYHA Class III, and LVEF range of 35–50%, 2- and 5-year mortality would be 32 and 57% in cases with HMR < 1.4, which are 4.5 and 3.6 times higher than that with HMR $\geq$ 2.0, respectively.

The present database from Japan included 70% non-ischaemic CHF and the remaining 30% ischaemic aetiology,[3] while ischaemic disease is more frequently responsible for CHF in Europe and the USA.[4,6] The incidence of cardiac death was similar for both ischaemic and non-ischaemic aetiologies, and CHF aetiology was not identified as a significant independent prognostic marker. Therefore, the prediction equations and risk models from this study can be used in any patient with CHF independent of underlying cardiac diseases. Prediction of mode of cardiac death was not possible, because the number of deaths in each category was insufficient to support further modelling. In other studies, ^{123}I-MIBG WR and LVEF have been shown to be predictors of life-threatening arrhythmias or SCD.[5] In ischaemic cardiomyopathy, sympathetic denervation

assessed using ^{11}C-hydroxyephedrine also predicted mortality from sudden cardiac arrest independently of LVEF and infarct volume (PAREPET study).[25]

The role of BNP and ^{123}I-MIBG may differ in clinical practice. Despite the limited number of BNP data, the Japanese pooled database analysis showed significant additive values of HMR to NYHA class and BNP.[3] In ADMIRE-HF study, addition of HMR did not significantly increase ROC curve AUCs for models including BNP using logistic analysis, but results only represented 2-year follow-up.[10] In the 5-year model of this study, combined use of BNP and HMR demonstrated better diagnostic power using ROC analysis, a finding not seen using the 2-year model. BNP is a simple blood test and can be repeatedly measured in routine practice. However, the level of this biomarker can rapidly change in response to patient conditions and treatment, indicating efficacies for tracking short-term outcomes and estimating the severity of CHF.[26] In contrast, ^{123}I-MIBG HMR changes more gradually during a several month period of clinical observation.[27] Thus, once BNP has stabilized, the HMR offers additional insight into the long-term prognosis, making the two tests complementary.

Most recent studies have indicated that an optimal HMR threshold for discriminating low from higher risk was between 1.6 and 1.8,[3,6,28] suggesting that impairment of cardiac sympathetic innervation contributes to lethal cardiac events irrespective of differences in clinical backgrounds and nationality. Thresholds of HMR in Japanese studies have been greater than those in European and North American studies, probably because of differences in specific activities of ^{123}I-MIBG and camera collimators used.[12] Recent studies using a cardiac phantom and various camera-collimator systems successfully showed the ability of a mathematical calibration method to cancel collimator-derived difference in HMR[12,29] and further clinical validation is required.

Single-photon emission computed tomographic (SEPCT) imaging with MIBG, which is widely performed to identify regional abnormalities of cardiac sympathetic innervation, was not available for the present study. Although SPECT method may be useful for localization of injured myocardium with arrhythmogenicity leading to lethal ventricular arrhythmias and SCD,[30] it is highly limited when cardiac MIBG activity is globally reduced as often seen in patients with advanced CHF and neurogenic disorders.[12] Thus, unlike for planar imaging, the appropriate role of cardiac MIBG SPECT imaging as a routine clinical tool in patients with CHF has yet to be established.

This study has several limitations. Because this study was an observational study using the multiple cohort database in which patients had been registered between 1990 and 2009, effects of contemporary drug and non-pharmacological device treatments on cardiac outcomes were not evaluated; only 11 patients underwent ICD therapy and 7 had CRT. Despite the size of this study, we could not confirm previous findings that showed that cardiac MIBG imaging identified patients at increased risk for appropriate ICD shocks against lethal arrhythmias or sudden death[31,32] and those likely to respond to CRT.[33] Because of the small number of patients undergoing the device treatment, occurrence of SCD was not affected by life-saving ICD shocks, indicating that the model reflects natural history and mortality risk without cardiac device treatment. For the further extrapolation of the presented findings to

European and North American populations, a large-scale, prospective study using patients undergoing treatment based on contemporary heart failure guidelines is needed to establish prognostic and therapeutic implications of cardiac ^{123}I-MIBG imaging and to determine how the technique can be used to identify high-risk patients most likely to benefit from device treatment in a cost-effective manner.

Conclusion

The 2- and 5-year risk models using four variables (NYHA class, age, LVEF, and cardiac sympathetic innervation parameter assessed by ^{123}I-MIBG) were developed for the calculation of cardiac mortality risk and for the identification of both low-risk and high-risk CHF patients. The incremental prognostic value of HMR in combination with BNP data was also documented. Application of risk charts to CHF patients can contribute to easy access to not only short-term but also long-term prognostication. Assessment of cardiac sympathetic innervation using ^{123}I-MIBG has the potential to assist clinicians in decision-making for the selection of risk-based therapeutic strategy, including appropriate use of cardiac devices.

References

1. Merlet P, Pouillart F, Dubois-Rande JL, Delahaye N, Fumey R, Castaigne A et al. Sympathetic nerve alterations assessed with 123I-MIBG in the failing human heart. J Nucl Med 1999;**40**:224–31.
2. Nakata T, Miyamoto K, Doi A, Sasao H, Wakabayashi T, Kobayashi H et al. Cardiac death prediction and impaired cardiac sympathetic innervation assessed by MIBG in patients with failing and nonfailing hearts. J Nucl Cardiol 1998;**5**:579–90.
3. Nakata T, Nakajima K, Yamashina S, Yamada T, Momose M, Kasama S et al. A pooled analysis of multicenter cohort studies of (123)I-mIBG imaging of sympathetic innervation for assessment of long-term prognosis in heart failure. JACC Cardiovasc Imaging 2013;**6**:772–84.
4. Verschure DO, Veltman CE, Manrique A, Somsen GA, Koutelou M, Katsikis A et al. For what endpoint does myocardial 123I-MIBG scintigraphy have the greatest prognostic value in patients with chronic heart failure? Results of a pooled individual patient data meta-analysis. Eur Heart J Cardiovasc Imaging 2014;**15**:996–1003.
5. Tamaki S, Yamada T, Okuyama Y, Morita T, Sanada S, Tsukamoto Y et al. Cardiac iodine-123 metaiodobenzylguanidine imaging predicts sudden cardiac death independently of left ventricular ejection fraction in patients with chronic heart failure and left ventricular systolic dysfunction: results from a comparative study with signal-averaged electrocardiogram, heart rate variability, and QT dispersion. J Am Coll Cardiol 2009;**53**:426–35.
6. Jacobson AF, Senior R, Cerqueira MD, Wong ND, Thomas GS, Lopez VA et al. Myocardial iodine-123 meta-iodobenzylguanidine imaging and cardiac events in heart failure. Results of the prospective ADMIRE-HF (AdreView Myocardial Imaging for Risk Evaluation in Heart Failure) study. J Am Coll Cardiol 2010;**55**:2212–21.
7. Nakata T, Wakabayashi T, Kyuma M, Takahashi T, Tsuchihashi K, Shimamoto K. Cardiac metaiodobenzylguanidine activity can predict the long-term efficacy of angiotensin-converting enzyme inhibitors and/or beta-adrenoceptor blockers in patients with heart failure. Eur J Nucl Med Mol Imaging 2005;**32**:186–94.
8. Toyama T, Aihara Y, Iwasaki T, Hasegawa A, Suzuki T, Nagai R et al. Cardiac sympathetic activity estimated by 123I-MIBG myocardial imaging in patients with dilated cardiomyopathy after beta-blocker or angiotensin-converting enzyme inhibitor therapy. J Nucl Med 1999;**40**:217–23.
9. Agostini D, Belin A, Amar MH, Darlas Y, Hamon M, Grollier G et al. Improvement of cardiac neuronal function after carvedilol treatment in dilated cardiomyopathy: a 123I-MIBG scintigraphic study. J Nucl Med 2000;**41**:845–51.
10. Narula J, Gerson M, Thomas GS, Cerqueira M, Jacobson AF. 123I mIBG imaging for prediction of mortality and potentially fatal events in heart failure: the ADMIRE-HFX Study. J Nucl Med 2015;**56**:1011–8.
11. Jacobson AF, Narula J. Introduction to cardiac neuronal imaging: a clinical perspective. J Nucl Med 2015;**56**(Suppl. 4):3S–6S.
12. Nakajima K, Nakata T. Cardiac 123I-MIBG Imaging for clinical decision making: 22-year experience in Japan. J Nucl Med 2015;**56**(Suppl. 4):11S–9S.
13. Nakajima K, Nakata T, Yamada T, Yamashina S, Momose M, Kasama S et al. A prediction model for 5-year cardiac mortality in patients with chronic heart failure using (123)I-metaiodobenzylguanidine imaging. Eur J Nucl Med Mol Imaging 2014;**41**:1673–82.
14. Wakabayashi T, Nakata T, Hashimoto A, Yuda S, Tsuchihashi K, Travin MI et al. Assessment of underlying etiology and cardiac sympathetic innervation to identify patients at high risk of cardiac death. J Nucl Med 2001;**42**:1757–67.
15. Yamada T, Shimonagata T, Fukunami M, Kumagai K, Ogita H, Hirata A et al. Comparison of the prognostic value of cardiac iodine-123 metaiodobenzylguanidine imaging and heart rate variability in patients with chronic heart failure: a prospective study. J Am Coll Cardiol. 2003;**41**:231–8.
16. Yamazaki J, Muto H, Kabano T, Yamashina S, Nanjo S, Inoue A. Evaluation of beta-blocker therapy in patients with dilated cardiomyopathy—Clinical meaning of iodine 123-metaiodobenzylguanidine myocardial single-photon emission computed tomography. Am Heart J 2001;**141**:645–52.
17. Momose M, Kobayashi H, Iguchi N, Matsuda N, Sakomura Y, Kasanuki H et al. Comparison of parameters of 123I-MIBG scintigraphy for predicting prognosis in patients with dilated cardiomyopathy. Nucl Med Commun 1999;**20**:529–35.
18. Matsui T, Tsutamoto T, Maeda K, Kusukawa J, Kinoshita M. Prognostic value of repeated 123I-metaiodobenzylguanidine imaging in patients with dilated cardiomyopathy with congestive heart failure before and after optimized treatments—comparison with neurohumoral factors. Circ J 2002;**66**:537–43.
19. Kasama S, Toyama T, Sumino H, Nakazawa M, Matsumoto N, Sato Y et al. Prognostic value of serial cardiac 123I-MIBG imaging in patients with stabilized chronic heart failure and reduced left ventricular ejection fraction. J Nucl Med 2008;**49**:907–14.
20. Imamura Y, Fukuyama T, Mochizuki T, Miyagawa M, Watanabe K, Ehime MHFSI. Prognostic value of iodine-123-metaiodobenzylguanidine imaging and cardiac natriuretic peptide levels in patients with left ventricular dysfunction resulting from cardiomyopathy. Jpn Circ J 2001;**65**:155–60.
21. Momose M, Okayama D, Nagamatsu H, Kondo C, Hagiwara N, Sakai S. Long-term prognostic stratification by a combination of (123)I-metaiodobenzylguanidine scintigraphy and ejection fraction in dilated cardiomyopathy. Ann Nucl Med 2011;**25**:419–24.
22. Doi T, Nakata T, Hashimoto A, Yuda S, Wakabayashi T, Kouzu H et al. Cardiac mortality assessment improved by evaluation of cardiac sympathetic nerve activity in combination with hemoglobin and kidney function in chronic heart failure patients. J Nucl Med 2012;**53**:731–40.
23. Ketchum ES, Jacobson AF, Caldwell JH, Senior R, Cerqueira MD, Thomas GS et al. Selective improvement in Seattle Heart Failure Model risk stratification using iodine-123 meta-iodobenzylguanidine imaging. J Nucl Cardiol 2012;**19**:1007–16.
24. Mozaffarian D, Anker SD, Anand I, Linker DT, Sullivan MD, Cleland JG et al. Prediction of mode of death in heart failure: the Seattle Heart Failure Model. Circulation 2007;**116**:392–8.

25. Fallavollita JA, Heavey BM, Luisi AJ Jr., Michalek SM, Baldwa S, Mashtare TL Jr. et al. Regional myocardial sympathetic denervation predicts the risk of sudden cardiac arrest in ischemic cardiomyopathy. *J Am Coll Cardiol* 2014;**63**:141–9.

26. Ito K, Kawai M, Nakane T, Narui R, Hioki M, Tanigawa S et al. Serial measurements associated with an amelioration of acute heart failure: an analysis of repeated quantification of plasma BNP levels. *Eur Heart J Acute Cardiovasc Care* 2012;**1**:240–7.

27. Kasama S, Toyama T, Iwasaki T, Sumino H, Kumakura H, Minami K et al. Evaluation of cardiac sympathetic nerve activity and aldosterone suppression in patients with acute decompensated heart failure on treatment containing intravenous atrial natriuretic peptide. *Eur J Nucl Med Mol Imaging* 2014;**41**:1683–91.

28. Agostini D, Verberne HJ, Burchert W, Knuuti J, Povinec P, Sambuceti G et al. I-123-mIBG myocardial imaging for assessment of risk for a major cardiac event in heart failure patients: insights from a retrospective European multicenter study. *Eur J Nucl Med Mol Imaging* 2008;**35**:535–46.

29. Nakajima K, Okuda K, Yoshimura M, Matsuo S, Wakabayashi H, Imanishi Y et al. Multicenter cross-calibration of I-123 metaiodobenzylguanidine heart-to-mediastinum ratios to overcome camera-collimator variations. *J Nucl Cardiol* 2014;**21**:970–8.

30. Boogers MJ, Borleffs CJ, Henneman MM, van Bommel RJ, van Ramshorst J, Boersma E et al. Cardiac sympathetic denervation assessed with 123-iodine metaiodobenzylguanidine imaging predicts ventricular arrhythmias in implantable cardioverter-defibrillator patients. *J Am Coll Cardiol* 2010;**55**: 2769–77.

31. Marshall A, Cheetham A, George RS, Mason M, Kelion AD. Cardiac iodine-123 metaiodobenzylguanidine imaging predicts ventricular arrhythmia in heart failure patients receiving an implantable cardioverter-defibrillator for primary prevention. *Heart* 2012;**98**:1359–65.

32. Nagahara D, Nakata T, Hashimoto A, Wakabayashi T, Kyuma M, Noda R et al. Predicting the need for an implantable cardioverter defibrillator using cardiac metaiodobenzylguanidine activity together with plasma natriuretic peptide concentration or left ventricular function. *J Nucl Med* 2008;**49**: 225–33.

33. Nishioka SA, Martinelli Filho M, Brandao SC, Giorgi MC, Vieira ML, Costa R et al. Cardiac sympathetic activity pre and post resynchronization therapy evaluated by 123I-MIBG myocardial scintigraphy. *J Nucl Cardiol* 2007;**14**:852–9.
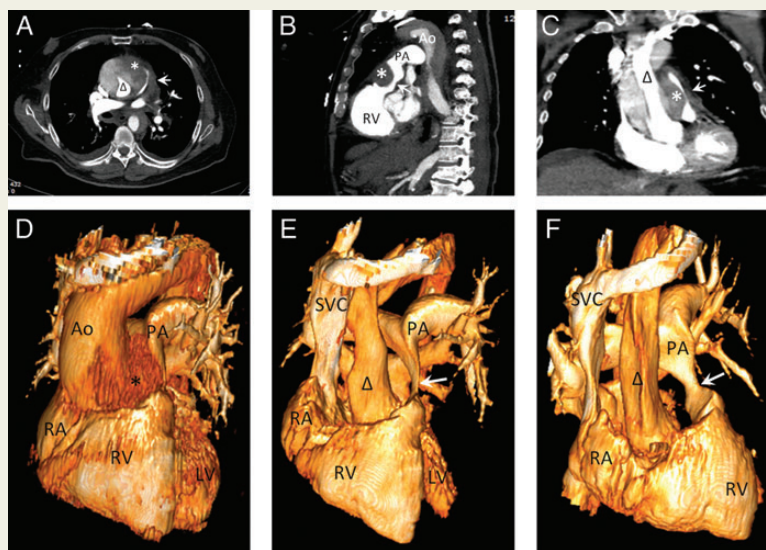
IMAGE FOCUS

Aortic dissection mimicking a massive pulmonary embolism

Eric J. Berkowitz[1], Itzhak Kronzon[1]*, James Whyburn[2], and Gila Perk[1]

[1]Department of Cardiovascular Disease, Northwell Health System, Lenox Hill Hospital, 100 East 77th Street, New York, NY, USA; and [2]Department of Radiology, Northwell Health System, Lenox Hill Hospital, New York, NY, USA

* Corresponding author. Tel: +212 434 6119; Fax: +212 434 2111. E-mail: kronzon@aol.com

An 85-year-old patient presented after an abrupt change in mentation and was found to be hypotensive and hypoxic. Transthoracic echocardiogram (TTE) (see Supplementary data online, *Video S1*) revealed an underfilled, hyperdynamic left ventricle (LV), and a dilated right ventricle (RV) with an akinetic free wall. Pulmonary artery systolic pressure (PASP) was estimated to be >70 mmHg. These findings, coupled with the clinical presentation, were highly suspicious of a massive pulmonary embolism (PE). A computed tomographic angiogram (CTA) (*Panels A–F*) was obtained which was negative for PE; however, it demonstrated a dissecting ascending aortic aneurysm with a contained rupture and haematoma formation (*Panels A–F*, asterisk), which was compressing the main pulmonary artery (PA) (*Panels A–F*, white arrow). These findings can be clearly visualized on 3D reconstructed volume rendered images (*Panels D–F*); post-processing removal of the false lumen of the aorta and the haematoma (asterisk), leaving in place the true lumen (white triangle), allows clear visualization of the externally compressed main PA (white arrow). After emergent surgery, the postoperative TTE demonstrated resolution of RV dilatation and function (see Supplementary data online, *Video S2*) with a normal PASP.

Compression of the PA from acute aortic dissection is extremely rare. Due to the aorta and pulmonary trunk sharing a common adventitia, a contained rupture of the ascending aorta into this shared space leads to haematoma formation, compressing the lumen of the PA. The subsequent presentation of these patients may mimic an acute massive PE, with all the coinciding findings on TTE.

Supplementary data are available at *European Heart Journal – Cardiovascular Imaging* online.